Proper chromosome alignment depends on BRCA2 phosphorylation by PLK1

Åsa Ehlén[1,2], Charlotte Martin[1,2†], Manon Julien[3,4†], Simona Miron[3†], François-Xavier Theillet[3], Virginie Boucherit[1,2], Patricia Duchambon[5,6], Ahmed El Marjou[5,7], Sophie Zinn-Justin[3], Aura Carreira[1,2*]

[1]Institut Curie, PSL Research University, CNRS, UMR3348, F-91405, Orsay, France

[2]Paris Sud University, Paris-Saclay University CNRS, UMR3348, F-91405 Orsay, France

[3]Institute for Integrative Biology of the Cell (I2BC), CEA, CNRS, Univ Paris-Sud, Université Paris-Saclay, Gif-sur-Yvette Cedex, France

[4]Department of Biology, École Normale Supérieure, 94230 Cachan, France
[5]Protein Expression and Purification Core Facility, Institut Curie, 26 rue d'Ulm, 75248 Paris Cedex 05, France
[6]INSERM U1196, 91405 Orsay Cedex, France
[7]CNRS UMR144, 12 rue Lhomond, 75005 Paris, France

[†] Equal contributors

[*]To whom correspondence should be addressed:
Aura Carreira
Institut Curie - Research Center
UMR 3348 CNRS "Genotoxic Stress and Cancer"
Bâtiment 110, Centre Universitaire
91405 Orsay
France
Phone: +33 (0)1 69 86 30 82
Fax: +33 (0)1 69 86 94 29
E-mail: aura.carreira@curie.fr

Summary

The BRCA2 tumor suppressor protein is involved in the maintenance of genome integrity through its role in homologous recombination (HR) in S/G2 phases of the cell cycle. A much less established function of BRCA2 takes place in mitosis where it interacts with the SAC component BUBR1 and plays a scaffold role in cytokinesis. BRCA2 is phosphorylated by the cell cycle regulator Polo-like kinase 1 (PLK1), so we asked whether this phosphorylation would have a role in the control of mitosis. Here we combined nuclear magnetic resonance spectroscopy, isothermal titration calorimetry and cell biology to characterize the phenotype of *BRCA2* variants that alter PLK1 phosphorylation. We identified T207 in BRCA2 as a *bona fide* docking site for PLK1 required for the phosphorylation of BUBR1 and the full alignment of the chromosomes at the metaphase plate. Precluding T207 binding to PLK1 as observed in *BRCA2* missense variants identified in breast cancer results in reduced phosphorylation of BUBR1 at PLK1-dependent sites and reducing the interaction of BUBR1 with the phosphatase PP2A-B56. This results in severe chromosome misalignment, chromosome segregation errors and aneuploidy. We thus reveal a direct mitotic role of BRCA2 in the alignment of chromosomes separate from its DNA repair function. These findings may explain in part the aneuploidy observed in *BRCA2*-deficient tumors.

Keywords

BRCA2; chromosome alignment; variants of uncertain significance (VUS); PLK1; phosphorylation; BUBR1; Mitosis; chromosome instability

Introduction

The BRCA2 tumor suppressor protein plays an important role in DNA repair by homologous recombination[1,2] which takes place preferentially during S/G2 phases of the cell cycle[3]. BRCA2 has also emerging functions in mitosis, for example, it binds to the spindle assembly component BUBR1[4], facilitating the acetylation/deacetylation of the latter[5,6], the function of which is poorly understood. At the end of mitosis, BRCA2 localizes to the midbody and facilitates cell division by serving as a scaffold protein for the central spindle components[7-9]. BRCA2 is a target of phosphorylation of PLK1 both in its N-terminal region[10] and in its central region[11], although the functional role of these phosphorylation events remains unclear.

PLK1 is a master regulator of the cell cycle, especially in mitosis[12,13]. Among other functions, PLK1 phosphorylates BUBR1 at several residues including the tension-sensitive sites S676[14] and T680[15] in prometaphase allowing the formation of stable kinetochore-microtubule attachments. This activity needs to be tightly regulated to ensure the proper alignment of the chromosomes at the metaphase plate[14,16,17]; in particular, Aurora B is an essential kinase that destabilizes erroneous kinetochore-microtubule interactions. The phosphatase PP2A-B56 protects initial kinetochore-microtubule interactions from excessive destabilization by Aurora B and this function is achieved through its interaction with BUBR1 phosphorylated at the Kinetochore Attachment and Regulatory Domain (KARD) motif (including residues S676 and T680) [15]. So, BUBR1, PLK1, Aurora B and PP2A-B56 are necessary for the formation of stable kinetochore-microtubule attachments.

PLK1 is recruited to specific targets via its Polo-box domain (PBD) [18]. PBD interacts with phosphosites characterized by the consensus motif S-[pS/pT]-P/X[19]. These

phosphosites are provided by a priming phosphorylation event, usually mediated by CDK1 or other proline-directed kinases[13]; however, there is also evidence that PLK1 itself might create docking sites ("self-priming") during cytokinesis [20,21].

Several BRCA2 sites corresponding to PLK1 consensus motifs have been identified as phosphorylated in mitosis, some of which belong to a cluster of predicted phosphosites located in BRCA2 N-terminus around residue S193[10]. We set out to investigate which of these sites are phosphorylated by PLK1, and to reveal whether these phosphorylation events play a role in the regulation of mitotic progression. Here, we demonstrate that T207 is a *bona fide* docking site for PLK1. By investigating the phenotype of BRCA2 missense variants that limit the phosphorylation of T207 by PLK1 we reveal an unexpected DNA-repair independent role of BRCA2 in the alignment of chromosomes at the metaphase plate. Furthermore, we demonstrate that this function is achieved by promoting the phosphorylation of the kinetochore tension-sensitive sites of BUBR1 by PLK1 which in turn facilitates the interaction of BUBR1 with the phosphatase PP2A-B56 required to counter excessive Aurora B activity at the kinetochores. A defect in this function of BRCA2 leads to chromosome instability manifested in chromosome misalignment, chromosome segregation errors and aneuploidy.

Results

BRCA2 variants identified in breast cancer reduce the PLK1-dependent phosphorylation of BRCA2 N-terminal region

Several missense variants of uncertain significance (VUS) identified in *BRCA2* in breast cancer patients are located in the region predicted to be phosphorylated by PLK1 (around S193) (Breast information core (BIC)[22] and BRCAshare [23]). To find out

if any of these variants affected PLK1 phosphorylation in this region, we purified fragments comprising amino acids 1 to 250 of BRCA2 (hereafter $BRCA2_{1-250}$) from HEK293T cells and used an *in vitro* kinase assay to assess the phosphorylation by PLK1 of the fragments containing either the WT sequence, the different BRCA2 variants M192T, S196N, T200K, S206C and T207A, or the mutant S193A, previously reported to reduce the phosphorylation of BRCA2 by PLK1[10] (Figure 1a, b). As expected, S193A reduced phosphorylation of $BRCA2_{1-250}$ by PLK1 (Figures 1a, 1b). Interestingly, variants T207A, S206C and T200K led to a 2-fold decrease in PLK1 phosphorylation of $BRCA2_{1-250}$ (Figure 1a, 1b). In contrast, M192T slightly increased the phosphorylation above WT levels whereas VUS S196N did not significantly modify the phosphorylation of $BRCA2_{1-250}$ by PLK1 (Figure 1a, b).

Together, these results show that VUS T207A, S206C and T200K identified in breast cancer patients impair phosphorylation of $BRCA2_{1-250}$ by PLK1 *in vitro*.

$BRCA2_{T207}$ is a target of phosphorylation by PLK1

The reduction of BRCA2 phosphorylation in $BRCA2_{1-250}$ containing T207A and S206C variants suggested that T207 could be a target of PLK1 phosphorylation. We investigated this possibility by following the PLK1 phosphorylation kinetics of a truncated fragment of BRCA2 N-terminus comprising T207 (amino acids 190-283) (hereafter $BRCA2_{190-283}$) by Magnetic Resonance (NMR) spectroscopy. NMR analysis allows residue-specific quantification of a peptide modification, provided it is ^{15}N-labelled. Figure 2a shows superimposed ^{1}H-^{15}N HSQC spectra of $BRCA2_{190-283}$ at different time points of the phosphorylation reaction with recombinant PLK1. Analysis of these experiments revealed phosphorylation of S193 and of eight other phosphosites, among which three threonines including T207 and five serines (Figure 2a). Four residues (T226>T207>T219>S193, Figure 2b, S1a) were favoured

phosphorylation sites, modified with markedly faster rates than the five other sites (S197, S217, S231, S239, S273). Interestingly, while T219 and T226 conservation is poor, T207 and S193 are conserved from mammals to fishes (Figures S1b and S1c) suggesting that both are important for BRCA2 function.

T207 phosphorylation together with the presence of a serine residue at position 206 creates a predicted docking site for $PLK1_{PBD}$[19]. Hence, we conclude that T207 is phosphorylated *in vitro* by PLK1, this phosphorylation is efficient in the context of $BRCA2_{190-283}$, and it may be a primary event for further BRCA2 phosphorylation via the recruitment of PLK1 to BRCA2.

BRCA2 variants T207A and T200K alter the phosphorylation kinetics of PLK1

Having identified T207 as a target of phosphorylation of PLK1, we next assessed the phosphorylation kinetics of T207 in the WT $BRCA2_{190-283}$ fragment and in the fragment containing the variants T207A or T200K that displayed reduced phosphorylation (Figure 1b, c). (The production of a ^{15}N recombinant fragment $BRCA2_{190-283}$ comprising S206C from bacteria yielded an insoluble protein precluding NMR analysis). Time-resolved NMR experiments revealed that PLK1 phosphorylates significantly less $BRCA2_{190-283}$ containing the variant T207A than the WT peptide (Figure 3a, 3b). Initial phosphorylation rates were decreased by a factor 5 (S193), 8 (T226) and 13 (T219) (Figure 3b, S2a). Variant T200K reduced by half the phosphorylation rates of S193, T207, T219 and T226 (Figures 3c, 3d and S2b).

In agreement with the *in vitro* kinase assay using the $BRCA2_{1-250}$ fragment purified from human cells (Figure 1), these results show that in $BRCA2_{190-283}$, variants T207A and T200K impair the phosphorylation of T207 and the cascade of associated phosphorylation events.

VUS T207A, S206C and T200K reduce the interaction of BRCA2 and PLK1

The finding that T207 is efficiently phosphorylated by PLK1 in $BRCA2_{190-283}$ polypeptide (Figure 2a) together with the observation that T207A mutation causes a global decrease in the phosphorylation of this region (Figure 3a) and the prediction that T207 is a docking site for $PLK1_{PBD}$ binding[19] made us hypothesize that T207 might be a "self-priming" phosphorylation event required for the interaction of PLK1 with BRCA2 at this site. If so, the variants that reduce phosphorylation of T207 by PLK1 would be predicted to alter $PLK1_{PBD}$ binding. To test this hypothesis, we examined the interaction of PLK1 with the VUS-containing polypeptides. Using an amylose pull-down, we overexpressed 2xMBP-$BRCA2_{1-250}$ constructs carrying these variants in U2OS cells and detected the bound endogenous PLK1 by western blotting. As expected, overexpressed $BRCA2_{1-250}$ was able to interact with endogenous PLK1 from mitotic cells but not from asynchronous cells (Figure 4a, lane 2 compared to lane 1). As previously described[10], mutation S193A reduced the binding to PLK1 (Figure 4a, lane 6 compared to lane 2). Interestingly, the variants reducing PLK1 phosphorylation (T207A, S206C and T200K) showed a weaker interaction with PLK1 than the WT protein (Figure 4a pull-down lane 4, 8 compared to lane 2 and lane 20 compared to lane 18) despite the protein levels of PLK1 being unchanged (Figure 4a, compare PLK1 input lanes 2, 4, 6, 8, 18, 20); in contrast, M192T and S196N did not affect the binding (Figure 4a, pull-down lane 12, 14 compared to lane 10). These results are consistent with the idea of a self-priming phosphorylation by PLK1 on T207.

T207 is a *bona fide* docking site for PLK1

To directly prove the recognition of pT207 by PLK1, we measured the affinity of recombinant $PLK1_{PBD}$ for a synthetic 17 aa peptide comprising phosphorylated T207. Using isothermal titration calorimetry (ITC), we found that recombinant $PLK1_{PBD}$ bound to the T207 phosphorylated peptide with an affinity of K_d= 0.09 ± 0.01 μM (Figure 4b), similar to the optimal affinity reported for an interaction between $PLK1_{PBD}$ and its phosphorylated target[19]. Consistently, $PLK1_{PBD}$ bound to the fragment $BRCA2_{190-283}$ with micromolar affinity upon phosphorylation by PLK1 (K_d= 0.14 ± 0.02 μM; Figure S3a) whereas it did not bind to the corresponding non-phosphorylated polypeptides (Figure 4c, Figure S3b). In agreement with the pull-down experiments, a peptide comprising mutated T207A abolished the interaction (Figure 4d). Importantly, a peptide comprising pT207 and S206C mutation could not bind to $PLK1_{PBD}$ (Figure 4e), as predicted from the consensus sequence requirement for $PLK1_{PBD}$ interaction[19]. Last, a peptide containing phosphorylated S197, which is also a predicted docking site for PLK1, bound with much less affinity to $PLK1_{PBD}$ than pT207 (K_d= 17 ± 2 μM; Figure S3c).

Taken together, these results indicate that phosphorylation of T207 by PLK1 promotes the interaction of PLK1 with BRCA2 through a *bona fide* docking site for PLK1 and favours a cascade of phosphorylation events. In variants T200K and T207A the decrease in T207 phosphorylation impairs PLK1 docking at T207 explaining the reduction of binding to PLK1 and the global loss of phosphorylation by PLK1. S206C eliminates the serine residue at -1 position required for $PLK1_{PBD}$ interaction resulting as well in a reduction of BRCA2 binding.

Impairing T207 phosphorylation prolongs mitosis

PLK1 is a master regulator of mitosis[13]. To find out whether the interaction between BRCA2 and PLK1 is involved in the control of mitotic progression we examined the functional impact of two of the variants that reduce PLK1 phosphorylation at T207 (S206C and T207A) in the context of the full-length BRCA2 protein in cells. For this purpose, we generated stable cell lines expressing the BRCA2 cDNA coding for either the WT or the variants to complement the DLD1 human cell line knock-out for *BRCA2*[24] (hereafter BRCA2$^{-/-}$). We selected two cell clones for each variant showing similar protein levels as the WT clone by western blot (Figure S4a). We then confirmed that the interaction of BRCA2 with PLK1 in cells expressing S206C and T207A was reduced compared to the WT BRCA2 expressing cells (Figure S4b) as shown for the BRCA2$_{1-250}$ fragment (Figure 4a).

To examine the impact of the cells expressing the variants on mitosis, we monitored by time-lapse microscopy the time that double-thymidine-synchronized individual cells from each clone spent in mitosis, from mitotic entry to daughter cell separation. Cells expressing the endogenous BRCA2 (hereafter BRCA2$^{+/+}$) and the WT clone showed similar kinetics, the majority of the cells (67% for BRCA2$^{+/+}$ and 83% for the WT clone) having completed mitosis within 60 min (Figure 5a, 5b). In contrast, cells expressing variants S206C and T207A augmented the time spent in mitosis as manifested by a significant decrease in the frequency of cells dividing within 60 min (~50%), similar to the BRCA2$^{-/-}$ cells (Figures 5a and 5b). In addition to a slower mitotic progression, S206C and T207A cells failed to divide with higher frequency than the WT complemented cells (14-23% compared to ~4% for the WT clone; Figure 5a, failure).

Taken together, cells expressing S206C and T207A display slower mitotic progression and higher frequency of mitotic failure compared to BRCA2 WT expressing cells.

Docking of PLK1 at T207 of BRCA2 is required for the phosphorylation of BUBR1 at T676 and S680 by PLK1 and to allow proper chromosome alignment

BRCA2 interacts directly with BUBR1[4,5]. BUBR1 associates with and is phosphorylated by PLK1, which controls the stability of kinetochore-microtubule interactions and enables the alignment of chromosomes at the metaphase plate[14,15]. The delay in mitotic progression observed in the clones expressing S206C and T207A (Figure 5a, b) led us to investigate BUBR1 levels in these cell lines. As previously described[14,25], upon cell arrest in G2/M phase, BUBR1 displayed 2 bands, the non-modified BUBR1 and the up-shifted band corresponding to phosphorylated BUBR1 (Figure 6a). Interestingly, the up-shifted band of BUBR1 strongly decreased in the cells expressing variants S206C or T207A compared to the cells expressing WT BRCA2 (Figure 6a, lane 4-6 compared to lane 2) and the same trend was observed in BRCA2$^{-/-}$ cells (Figure 6a, lane 8 compared to lane 10). To find out the species of BUBR1 altered in the stable cells expressing the variants, we probed the same membrane with an antibody specific for pT680, a known BUBR1 target phosphosite for PLK1[15]. Interestingly, both clones of the cells expressing variants S206C and T207A displayed reduced pT680 levels of BUBR1 (Figure 6a). As previously described[15], the phosphorylation of T680 is mediated by PLK1 since PLK1 inhibitors strongly reduced this signal (Figure S5a) and phosphatase treatment resulted in a decrease of the intensity of the band (Figure S5b). Furthermore, we observed a reduction in the PLK1-dependent phosphorylation of S676, another

known target site of PLK1 in BUBR1[14] (Figure 6b), indicating that BUBR1 phosphorylation by PLK1 is impaired in these cells at least at these two sites.

BUBR1 also facilitates kinetochore-microtubules attachment via its interaction with the phosphatase PP2A-B56 which requires the phosphorylation of BUBR1 at the KARD motif[15]. This domain comprises S676 and T680 phosphorylated by PLK1 so we next tested whether the interaction of BUBR1 with PP2A-B56 was altered in cells that reduce BUBR1 phosphorylation by PLK1. As expected, PP2A-B56 was pulled-down with BUBR1 immunoprecipitated from mitotic cell lysates expressing WT BRCA2 as detected by an antibody against the catalytic subunit of PP2A (PP2AC). In contrast, the interaction with PP2A-B56 was very much reduced in cells expressing T207A (Figure 6c).

The phosphorylation of BUBR1 at T676 and S680 by PLK1 and its association with PP2A-B56 are required for the formation of stable kinetochore-microtubules attachments[14,15], a defect of which results in chromosome misalignment. Therefore, we next examined whether cells expressing the BRCA2 variants S206C and T207A that showed reduced levels of pT680 and pS676-BUBR1 altered chromosome alignment.

Following thymidine synchronization, the cells were blocked in prometaphase with Monastrol and then treated with proteasome inhibitor MG132 for 1h to avoid exit from mitosis. Chromosome alignment was subsequently analysed by immunofluorescence. Strikingly, analysis of cells expressing S206C and T207A variants showed high frequency of faulty chromosome congression compared to the WT BRCA2 clone (52% in S206C A9, 42.4% in T207 B1 versus 15.8% in the WT clone) (Figure 6d, e) as detected by a signal of the centromere marker (CREST) outside the metaphase plate (Figure 6e). Interestingly, most of the misaligned

chromosomes were characterized by a very slow chromosome capture leading to chromosomes located close to the spindle pole as revealed by the colocalization of CREST with the microtubule marker α-tubulin (Figure 6e, 6e).

Together, our results show that the phosphorylation of BUBR1 by PLK1 is impaired in cells expressing the variants of BRCA2 that cannot recruit PLK1 at T207 suggesting that PLK1 needs to be bound to BRCA2 to efficiently phosphorylate BUBR1. The impaired phosphorylation of BUBR1 decreases its interaction with PP2A-B56 and as a consequence, these cells display severe chromosome misalignments.

The BRCA2 variants that reduce PLK1 phosphorylation display a weaken SAC activity, strong defects in chromosome segregation and aneuploidy

BUBR1 is an essential component of the SAC[26] ensuring proper chromosome segregation. In view of the interaction of BRCA2 with BUBR1[4,5] and the impact of BRCA2 on BUBR1 phosphorylation (Figure 6a), we next assessed the SAC activity by measuring the percentage of cells arrested in mitosis after treatment with the spindle poison nocodazole (Figure 7a), using phosphorylated (S10) histone 3 (pH3) as a mitotic marker[27]. As expected, upon nocodazole treatment, the percentage of pH3 positive WT cells increased compared to non-treated cells, this increase was similar to the one observed in cells expressing endogenous BRCA2 ($BRCA2^{+/+}$) whereas in BRCA2 deficient cells ($BRCA2^{-/-}$) the percentage was significantly lower (Figure 7a). Interestingly, the stable cell lines expressing variants S206C and T207A showed a significant decrease in the percentage of mitotic cells after nocodazole treatment in comparison to the WT BRCA2 cells, indicating a weaken SAC activity under mitotic-arrested conditions (Figure 7a). Consistently, a smaller percentage of G2/M cells was observed in S206C and T207A clones compared to the WT clone

upon mitotic arrest induction (Figure S6a). The reduced number of cells in G2/M was not due to a defective cell cycle profile as the distribution of these cells in non-induced conditions was equivalent to that of the WT cells (Figure S6b).
Thus, in response to microtubule poison, VUS S206C and T207A compromise SAC activity, which results in a weaken ability to induce mitotic arrest.

Unresolved chromosome misalignment as observed in these cells together with a weaken SAC activity is expected to drive chromosome missegregation. To find out if this was the case in cells expressing S206C and T207A variants we next examined these cells synchronized by double-thymidine block at anaphase/telophase. As quantified in Figure 7b and illustrated in Figure 7c, 65% of cells expressing S206C and 50% of T207A variants displayed chromosome segregation errors including lagging chromosomes and chromosome bridges compared to 29% in the WT expressing cells.

Erroneous chromosome segregation generates aneuploid cells during cell division[28]. Given the strong chromosome segregation defect observed in cells expressing S206C and T207A we next analysed the number of chromosomes in the same cells. Total chromosome counts carried out on metaphase spreads revealed that 34% of WT BRCA2 clone exhibited aneuploidy with chromosome loss or gain. In the case of S206C A7 and T207A B1, this number was significantly elevated to 47% and 60% of the cells, respectively (Figure 7d, e).

Together, these results indicate that, in addition to the severe chromosome misalignment, cells expressing S206C and T207A display a weaken SAC activity upon induced mitotic arrest leading to high frequency of chromosome

missegregation. As a consequence, the incidence of aneuploidy is greatly exacerbated in these cells.

The BRCA2 variants altering PLK1 phosphorylation restore the hypersensitivity of BRCA2 deficient cells to DNA damage or PARP inhibition

Since BRCA2 has a major role in DNA repair by homologous recombination (HR), the prolonged mitosis observed in the VUS-expressing cell lines (Figure 5) could result from checkpoint activation through unrepaired DNA. In addition, defects in chromosome segregation have been reported as a cause of DNA damage[29]. To test the DNA repair efficiency of the cell lines expressing VUS S206C and T207A, we performed a clonogenic survival assay in the stable clones treated with mitomycin C (MMC), an inter-strand crosslinking agent to which BRCA2 deficient cells are highly sensitive[30]. As expected, BRCA2 deficient cells ($BRCA2^{-/-}$) showed hypersensitivity to MMC treatment whereas BRCA2 WT cells complemented this phenotype almost to the same survival levels as the cells expressing the endogenous BRCA2 ($BRCA2^{+/+}$), validating our cell system. The stable clones expressing VUS S206C and T207A also complemented the hypersensitive phenotype of BRCA2 deficient cells ($BRCA2^{-/-}$) reaching similar levels as the WT clone (WT C1) (Figure 8a) suggesting that the delay in mitosis is not a consequence of checkpoint activation via unrepaired DNA. In contrast, clones expressing VUS S206C and T207A did show a growth defect manifested in a reduced number of colonies observed in unchallenged cells (Figure S6c), which is consistent with the mitotic delay observed by video-microscopy (Figure 5). To more specifically address the DNA repair activity of these cells, we then tested the viability of the same cells grown in the presence of the poly (ADP-ribose) polymerase (PARP) inhibitor Olaparib. PARP1 is an enzyme required for the sensing

of SSB and DSBs that becomes essential in the absence of a functional HR pathway [31] and therefore is used as a surrogate of HR proficiency. Indeed, PARP1 inhibitors, in particular Olaparib, is currently used in the clinic to treat breast and ovarian cancer patients carrying germline mutations in BRCA1/2. In our settings, the relative viability of $BRCA2^{-/-}$ cells was 45% upon treatment with the highest Olaparib concentration tested (5 μM), in contrast to 74% viability for the WT complemented cells. Similarly, cells expressing S206C or T207A survived the treatment equally well as the cells expressing WT BRCA2, the percentage of viable cells at 5 μM treatment ranging from 70 to 83 % depending on the clone (Figure 8b). Furthermore, we tested whether the interaction of BRCA2 and PLK1 was affected by DNA damage treatment. We immunoprecipitated overexpressed $BRCA2_{1-250}$ WT fragment from whole cell extracts of mitotic arrested cells exposed to ionizing radiation (IR) and checked the amount of PLK1 pulled-down in these cells. As previously reported[32], the exposure to IR did not alter the amount of PLK1 bound to BRCA2 in our cell lines (Figure S6d).

In summary, these results indicate that the role of BRCA2 in conjunction with PLK1 in mitosis is independent of the homologous recombination function of BRCA2.

Discussion

Our results demonstrate that residues S193 and T207 of BRCA2 can be phosphorylated by PLK1 (Figure 2) and that pT207 constitutes a *bona fide* docking site for $PLK1_{PBD}$ (Figure 4b). Accordingly, *BRCA2* missense variants of unknown clinical significance reducing the phosphorylation status of T207 (T207A, S206C, T200K), result in a decrease in the interaction of BRCA2-PLK1 (Figure 4 and S4b). The phenotype of cells expressing two of these variants (S206C, T207A) in the context of the full-length protein in BRCA2 deficient background, allowed us to

investigate in detail the possible role of BRCA2 phosphorylation by PLK1 in the control of mitosis. Unexpectedly, we found that the cells expressing BRCA2 missense breast cancer variants that preclude the docking of PLK1 at T207 display defective chromosome congression to the metaphase plate (Figure 6d, e). Remarkably, variants S206C and T207A of BRCA2 lead to a frequency of chromosome misalignment equivalent to the one reported for BUBR1 mutated in the three phosphorylation targets sites of PLK1, BUBR1 3A mutant[15].

Mechanistically, cells expressing T207A and S206C exhibit reduced PLK1-dependent BUBR1 phosphorylation at two known tension-sensitive phosphosites required for the establishment of kinetochore-microtubule attachments, S676 and T680[14,15] (Figure 6a, b). Importantly, these results strongly suggest that the recruitment of PLK1 at pT207 docking site in BRCA2 is required for the phosphorylation of BUBR1 by PLK1. Proper kinetochore-microtubule attachments also require the interaction of BUBR1 with the phosphatase PP2A-B56 to balance Aurora B kinase activity[15,33]. This interaction is mediated through the KARD motif of BUBR1 phosphorylated by PLK1. As expected from a reduction in BUBR1 phosphorylation, cells expressing T207A reduce the binding of BUBR1 to PP2A-B56 (Figure 6c) suggesting that the phenotype of these cells is due to an improper balance of kinase-phosphatases.

The increased chromosome misalignment leads to mitotic delay (Figure 5), which is indicative of a functional SAC. However, upon induced mitotic arrest these cells display weaken SAC activity as manifested in a reduced frequency of mitotic cells (Figure 7a) implying that the mitotic checkpoint is not fully activated, as expected from a defective function of BUBR1[17,26,34]. These results explain the chromosome segregation errors observed in these cells (7a, b). Importantly, the faulty segregation

led to the development of aneuploidy in cells expressing T207A and S206C.

Finally, the activity of BRCA2-PLK1 interaction in mitotic progression is independent of the HR function of BRCA2 as cells expressing these VUS display normal sensitivity to DNA damage and viability in the presence of PARP inhibitors (Figure 8a,b).

Putting our results together we propose the following model (Figure 8c): In cells expressing WT BRCA2, PLK1 phosphorylates BRCA2 on T207 leading to the docking of PLK1 at this site. This step promotes the phosphorylation of BUBR1 at the tension-sensitive phosphosites (T676 and S680) by PLK1 in prometaphase allowing the interaction of BUBR1 with the phosphatase PP2A-B56 to balance Aurora B activity (Figure 8c, panel 1). Once the kinetochore-microtubules attachments are established and proper tension is achieved, BUBR1 is no longer phosphorylated by PLK1[14]. This leads to a full alignment of chromosomes at the metaphase plate (Figure 8c, panel 2) and the subsequent faithful chromosome segregation in anaphase (Figure 8c, panel 3).

In cells expressing the variants that fail to be phosphorylated at T207 (T200K, S206C, T207A) PLK1 cannot be recruited to pT207, impairing the phosphorylation of BUBR1 by the same kinase (Figure 8c, panel 1'), reducing PP2A-B56 interaction, thus leading to misalignment defects that prolong mitosis (Figure 8c, panel 2'). This may also unbalance the pool of BUBR1 required for SAC activation as cells carrying these variants display weaken SAC response only upon treatment with microtubule poison (Figure 7a); as a consequence, these cells exhibit increased chromosome segregation errors (Figure 8c, panel 3') and aneuploidy. The phenotype we observe in these clones fits very well with the presence of two pools of BUBR1 as recently

described[17], one that is important for chromosome alignment onto the metaphase plate, and another that activates the SAC.

Our results are consistent with the "processive phosphorylation" model (as opposed to the "distributive phosphorylation" model) proposed before on how $PLK1_{PBD}$ regulates the kinase activity of PLK1[35], with some modifications. In this model, $PLK1_{PBD}$ would first bind the site phosphorylated by another mitotic kinase allowing the kinase domain of PLK1 to phosphorylate the same protein at another site. In this work, we show that the mitotic kinase would be PLK1 itself ("self-priming"[21]), and the kinase domain of PLK1 would phosphorylate not the same protein but BUBR1 bound to BRCA2. Interestingly, the consensus sequence of PLK1 phosphorylation imposes an aspartic or glutamic acid at the -1 position instead of a serine (S206)[36]. Thus, this work extends the consensus sequence of PLK1 phosphorylation.

In all, we reveal an unexpected chromosome stability control mechanism that depends on the interaction and phosphorylation of BRCA2 by PLK1 that ensures the efficient phosphorylation of BUBR1 by the same kinase required for PP2A-B56 interaction and the proper balance of kinases and phosphatases at the kinetochore. This mechanism is required for the faithful segregation of DNA content to daughter cells, a function that is separate from the HR activity of BRCA2.

BRCA2 harbours another docking site for PLK1 at T77, a site that is primed by CDK phosphorylation[32]. In this study we observed, in addition to T207, several phosphorylation events including S193 (Figure 2) which is required for the midbody localization of BRCA2[9]. Furthermore, other PLK1-phosphorylation sites have been described in the central region of BRCA2[11]. However, the chronology of phosphorylation events throughout the cell cycle and how they are coordinated

deserves further study.

The fact that *BRCA2* missense variants identified in breast cancer patients affect BRCA2 phosphorylation by PLK1 with direct consequences in chromosome stability manifested by chromosome missegregation and aneuploidy strongly suggests that this function could be associated with the aneuploidy observed in *BRCA2*-deficient tumors[37]. Moreover, the lack of sensitivity to the PARP inhibitor Olaparib have important clinical implications, as breast cancer patients carrying these variants are not predicted to respond to this type of treatment unlike *BRCA2*-mutated tumors that are HR-deficient.

Author Contributions

A.E. purified WT and mutated $BRCA2_{1-250}$, established the stable $DLD1^{-/-}$ cell lines, performed kinase assays, pull-down assays, western blots, time-lapse microscopy experiments, mitotic index measurements by FACS and clonogenic survival assays as well as the statistical analysis for these experiments. C.M. performed IF and image acquisition of metaphase plate alignment, chromosome segregation and karyotype analysis. M.J. performed the NMR experiments assisted by S. M., F.T. and S.Z.J. S.M. performed the ITC experiments and purified $PLK1_{PBD}$. V.B. assisted establishing stable clones and performing clonogenic survival assays. P.D. purified $PLK1_{PBD}$. A.M. cloned and produced PLK1 from insect cells. A.C., A.E. and S.Z.J. designed the experiments. A.C. and S.Z.J. supervised the work. A.C. wrote the paper with important contributions from all authors.

Acknowledgments

We thank members of the AC lab for fruitful comments on the manuscript and Davide Panigada for the illustration of chromosomes in Figure 8. We thank Rene H. Medema and Marie Dutreix for useful discussions on this work. We also thank Juan S. Martinez for construct BRCA2$_{1-250}$ and Eric Nigg for pS676-BUBR1 antibody. We acknowledge the Cell and Tissue Imaging Facility of the Institut Curie (PICT), a member of the France BioImaging National Infrastructure (ANR-10-INBS-04) and the French Infrastructure for Integrated Structural Biology (https://www.structuralbiology.eu/networks/frisbi, (ANR-10-INSB-05-01).

This work was supported by the ATIP-AVENIR CNRS/INSERM Young Investigator grant 201201, EC-Marie Curie Career Integration grant CIG293444 to A.C. and Institut National du Cancer INCa-DGOS_8706 to A.C. and S.Z.J.; A.E. was supported by the Swedish Society for Medical Research.

The authors declare no conflict of interest.

Correspondence and requests for materials should be addressed to A.C.

References

1. Moynahan, M. E., Pierce, A. J. & Jasin, M. BRCA2 is required for homology-directed repair of chromosomal breaks. *Molecular Cell* **7,** 263–272 (2001).
2. Jensen, R. B., Carreira, A. & Kowalczykowski, S. C. Purified human BRCA2 stimulates RAD51-mediated recombination. *Nature* **467,** 678–683 (2010).
3. Saleh-Gohari, N. & Helleday, T. Conservative homologous recombination preferentially repairs DNA double-strand breaks in the S phase of the cell cycle in human cells. *Nucleic Acids Research* **32,** 3683–3688 (2004).
4. Futamura, M. *et al.* Potential role of BRCA2 in a mitotic checkpoint after phosphorylation by hBUBR1. *Cancer Res* **60,** 1531–1535 (2000).
5. Choi, E. *et al.* BRCA2 fine-tunes the spindle assembly checkpoint through reinforcement of BubR1 acetylation. *Developmental Cell* **22,** 295–308 (2012).
6. Park, I. *et al.* HDAC2/3 binding and deacetylation of BubR1 initiates spindle assembly checkpoint silencing. *FEBS J* (2017). doi:10.1111/febs.14286

7. Mondal, G. *et al.* BRCA2 localization to the midbody by filamin A regulates cep55 signaling and completion of cytokinesis. *Developmental Cell* **23,** 137–152 (2012).
8. Daniels, M. J., Wang, Y., Lee, M. & Venkitaraman, A. R. Abnormal cytokinesis in cells deficient in the breast cancer susceptibility protein BRCA2. *Science* **306,** 876–879 (2004).
9. Takaoka, M., Saito, H., Takenaka, K., Miki, Y. & Nakanishi, A. BRCA2 phosphorylated by PLK1 moves to the midbody to regulate cytokinesis mediated by nonmuscle myosin IIC. *Cancer Res* **74,** 1518–1528 (2014).
10. Lin, H.-R., Ting, N. S. Y., Qin, J. & Lee, W.-H. M phase-specific phosphorylation of BRCA2 by Polo-like kinase 1 correlates with the dissociation of the BRCA2-P/CAF complex. *J Biol Chem* **278,** 35979–35987 (2003).
11. Lee, M., Daniels, M. J. & Venkitaraman, A. R. Phosphorylation of BRCA2 by the Polo-like kinase Plk1 is regulated by DNA damage and mitotic progression. *Oncogene* **23,** 865–872 (2004).
12. Zitouni, S., Nabais, C., Jana, S. C., Guerrero, A. & Bettencourt-Dias, M. Polo-like kinases: structural variations lead to multiple functions. *Nat Rev Mol Cell Biol* **15,** 433–452 (2014).
13. Barr, F. A., Silljé, H. H. W. & Nigg, E. A. Polo-like kinases and the orchestration of cell division. *Nat Rev Mol Cell Biol* **5,** 429–440 (2004).
14. Elowe, S., Hümmer, S., Uldschmid, A., Li, X. & Nigg, E. A. Tension-sensitive Plk1 phosphorylation on BubR1 regulates the stability of kinetochore microtubule interactions. *Genes Dev* **21,** 2205–2219 (2007).
15. Suijkerbuijk, S. J. E., Vleugel, M., Teixeira, A. & Kops, G. J. P. L. Integration of kinase and phosphatase activities by BUBR1 ensures formation of stable kinetochore-microtubule attachments. *Developmental Cell* **23,** 745–755 (2012).
16. Elowe, S. *et al.* Uncoupling of the spindle-checkpoint and chromosome-congression functions of BubR1. *J Cell Sci* **123,** 84–94 (2010).
17. Zhang, G., Mendez, B. L., Sedgwick, G. G. & Nilsson, J. Two functionally distinct kinetochore pools of BubR1 ensure accurate chromosome segregation. *Nature Communications* **7,** 12256 (2016).
18. Elia, A. E. H., Cantley, L. C. & Yaffe, M. B. Proteomic screen finds pSer/pThr-binding domain localizing Plk1 to mitotic substrates. *Science* **299,** 1228–1231 (2003).
19. Elia, A. E. H. *et al.* The molecular basis for phosphodependent substrate targeting and regulation of Plks by the Polo-box domain. *Cell* **115,** 83–95 (2003).
20. Neef, R. *et al.* Phosphorylation of mitotic kinesin-like protein 2 by polo-like kinase 1 is required for cytokinesis. *J Cell Biol* **162,** 863–875 (2003).
21. Kang, Y. H. *et al.* Self-regulated Plk1 recruitment to kinetochores by the Plk1-PBIP1 interaction is critical for proper chromosome segregation. *Mol. Cell* **24,** 409–422 (2006).
22. Szabo, C., Masiello, A., Ryan, J. F. & Brody, L. C. The breast cancer information core: database design, structure, and scope. *Hum. Mutat.* **16,** 123–131 (2000).
23. Béroud, C. *et al.* BRCA Share: A Collection of Clinical BRCA Gene Variants. *Hum. Mutat.* **37,** 1318–1328 (2016).

24. Hucl, T. *et al.* A syngeneic variance library for functional annotation of human variation: application to BRCA2. *Cancer Res* **68,** 5023–5030 (2008).
25. Huang, H. *et al.* Phosphorylation sites in BubR1 that regulate kinetochore attachment, tension, and mitotic exit. *The Journal of Cell Biology* **183,** 667–680 (2008).
26. Sudakin, V., Chan, G., biology, T. Y. T. J. O. C.2001. Checkpoint inhibition of the APC/C in HeLa cells is mediated by a complex of BUBR1, BUB3, CDC20, and MAD2. T*he Journal of Cell Biology* **154,** 925-936 (2001).
27. Giet, R. & Glover, D. M. Drosophila Aurora B Kinase Is Required for Histone H3 Phosphorylation and Condensin Recruitment during Chromosome Condensation and to Organize the Central Spindle during Cytokinesis. *J Cell Biol* **152,** 669–682 (2001).
28. Santaguida, S. & Amon, A. Short- and long-term effects of chromosome mis-segregation and aneuploidy. *Nat Rev Mol Cell Biol* **16,** 473–485 (2015).
29. Janssen, A., van der Burg, M., Szuhai, K., Kops, G. J. P. L. & Medema, R. H. Chromosome Segregation Errors as a Cause of DNA Damage and Structural Chromosome Aberrations. *Science* **333,** 1895–1898 (2011).
30. Kraakman-van der Zwet, M. *et al.* Brca2 (XRCC11) deficiency results in radioresistant DNA synthesis and a higher frequency of spontaneous deletions. *Mol. Cell. Biol.* **22,** 669–679 (2002).
31. Bryant, H. E. *et al.* Specific killing of BRCA2-deficient tumours with inhibitors of poly(ADP-ribose) polymerase. *Nature* **434,** 913–917 (2005).
32. Yata, K. *et al.* BRCA2 coordinates the activities of cell-cycle kinases to promote genome stability. *CellReports* **7,** 1547–1559 (2014).
33. Foley, E. A., Maldonado, M. & Kapoor, T. M. Formation of stable attachments between kinetochores and microtubules depends on the B56-PP2A phosphatase. *Nat Cell Biol* **13,** 1265–1271 (2011).
34. Musacchio, A. & Salmon, E. D. The spindle-assembly checkpoint in space and time. *Nat Rev Mol Cell Biol* **8,** 379–393 (2007).
35. Lowery, D. M., Lim, D. & Yaffe, M. B. Structure and function of Polo-like kinases. *Oncogene* **24,** 248–259 (2005).
36. Nakajima, H., Toyoshima-Morimoto, F., Taniguchi, E. & Nishida, E. Identification of a consensus motif for Plk (Polo-like kinase) phosphorylation reveals Myt1 as a Plk1 substrate. *J Biol Chem* **278,** 25277–25280 (2003).
37. Gretarsdottir, S. *et al.* BRCA2 and p53 Mutations in Primary Breast Cancer in Relation to Genetic Instability. *Cancer Res* **58,** 859–862 (1998).

Figure legends

Figure 1. BRCA2 VUS alter PLK1 phosphorylation of $BRCA2_{1-250}$

(a) PLK1 *in vitro* kinase assay with $BRCA2_{1-250}$. Top: The polypeptides encompassing $BRCA2_{1-250}$ WT or S193A, M192T, S196N, T200K, S206C, T207A

mutations were incubated with recombinant PLK1 in the presence of γ^{32}P-ATP. The samples were resolved on 7.5% SDS-PAGE and the ^{32}P-labeled products were detected by autoradiography. Bottom: 7.5% SDS-PAGE showing the input of purified 2xMBP-BRCA2$_{1-250}$ WT and mutated proteins (0.5 μg) used in the reaction as indicated. **(b)** Quantification of the relative phosphorylation in (a). Data in (b) are represented as mean ± SD from at least three independent experiments (WT (n=9), S193A (n=4), M192T (n=4), S196N (n=4), S206C (n=4), T200K (n=5), T207A (n=4)). One-way ANOVA test with Tukey's multiple comparisons test was used to calculate statistical significance of differences (the asterisks show differences compared to WT; ns (non-significant), $p > 0.05$, * $p \leq 0.05$, ** $p \leq 0.01$, *** $p \leq 0.001$).

Figure 2. PLK1 phosphorylates T207 in BRCA2$_{190-283}$

Phosphorylation kinetics of BRCA2$_{190-283}$ as observed by NMR. **(a)** Superposition of the ^{1}H-^{15}N HSQC spectra recorded as a function of the phosphorylation time: from black (before phosphorylation) to red (after 24h with PLK1). PLK1 (1.1 μM) was incubated with ^{15}N labelled BRCA2$_{190-283}$ (200 μM) at 30°C and 200 μl were taken for each time point. Right panel: Zoom on the region containing the NMR signals of the phosphorylated residues. NMR peaks are labelled to indicate the corresponding residue following the timing colour code indicated in the left arrow (dark blue label: peaks appearing before 4 h; green label: peaks appearing before 5 h; red label: peaks observed only at 24 h). pT219 and pT226 give rise to several peaks (marked as (a), (b), (c)) as a function of the phosphorylation state of the surrounding residues. **(b)** Phosphorylation kinetics of S193 (red), T207 (black), T219 (blue) and T226 (grey). In the case of T226, the phosphorylation percentage corresponds to the sum of the intensities of peaks pT226(a), pT226(b) and pT226(c), which reflects the

existence of different environments for phosphorylated T226 due to further phosphorylation of neighbouring T219 and S231. The multiplicity of the peaks corresponding to phosphorylated T226 at 24h hindered a proper measurement of this time point.

Figure 3. BRCA2 VUS alter PLK1 phosphorylation of BRCA2$_{190-283}$

(a) Superposition of the ^{1}H-^{15}N HSQC spectra recorded on VUS T207A as a function of the phosphorylation time: from black (before phosphorylation) to red (after 24h incubation with PLK1). The conditions are the same as in Figure 2a. A zoom on the region containing the NMR signals of the phosphorylated residues is shown. **(b)** Phosphorylation kinetics of T207 (black), S193 (red), T226 (grey) and T219 (blue), in WT (filled circles) versus T207A mutated BRCA2$_{190-283}$ (empty circles). **(c)** Superposition of the ^{1}H-^{15}N HSQC spectra recorded on variant T200K as a function of the phosphorylation time. **(d)** Phosphorylation kinetics of T207 (black), S193 (red), T226 (grey) and T219 (blue), in WT (filled circles) versus T200K mutated BRCA2$_{190-283}$ (empty circles).

Figure 4. BRCA2 variants showing reduced phosphorylation by PLK1 impair PLK1 binding

(a) 2xMBP-BRCA2$_{1-250}$ expressing the WT, the VUS (M192T, S196N, T200K, S206C and T207A) or the mutant S193A were expressed in U2OS cells by transient transfection for 30h before the cells were treated with nocodazole for 14h. Mitotic cells were lysed and immunoprecipitation was performed against the MBP tag using amylose beads. Complexes were resolved on 4-15% SDS-PAGE followed by western blotting using anti-PLK1 and anti-MBP antibodies. **(b-e)** Isothermal Titration

Calorimetry (ITC) thermograms showing binding of $PLK1_{PBD}$ to a 17 aa BRCA2 peptide containing **(b)** pT207, **(c)** T207, **(d)** A207, **(e)** C206pT207.

Figure 5. BRCA2 variants S206C and T207A prolong mitosis

(a) Top: Scheme of the double thymidine block procedure used to synchronize DLD1 cells expressing endogenous BRCA2 ($BRCA2^{+/+}$) or stable clones of BRCA2 deficient DLD1 cells ($BRCA2^{-/-}$) expressing GFPMBP-BRCA2 WT or the variants S206C or T207A for live-cell imaging of cells progressing through mitosis. Bottom: Frequency distribution of the time cells spend in mitosis from anaphase onset to daughter cell separation monitored by time-lapse microscopy. ($BRCA2^{+/+}$ (n=3), $BRCA2^{-/-}$ (n=4), WT C1 (n=6), S206C A7 and A9 (n=3), T207A B1 and E4 (n=3)). **(b)** Representative still images of the live-cell imaging performed in Figure 5a at different time points. The numbers in each image indicates the time in min after mitotic onset. Scale bar represents 10 µm. Statistical significance of the difference in (a) was calculated with two-way ANOVA test with Tukey's multiple comparisons test (the asterisks show differences compared to WT; ns (non-significant), $p > 0.05$, * $p \leq 0.05$, ** $p \leq 0.01$, *** $p \leq 0.001$, **** $p \leq 0.0001$).

Figure 6. Cells expressing BRCA2 variants that alter PLK1 phosphorylation display reduced protein levels of phosphorylated BUBR1, reducing its interaction with PP2A-B56 resulting in chromosomes misalignment

(a, b) Western blots showing the expression levels of endogenous BUBR1 and (a) pT680-BUBR1 or (b) pS676-BUBR1 in nocodazole treated or untreated DLD1 cells expressing endogenous BRCA2 ($BRCA2^{+/+}$) or stable clones of DLD1 BRCA2 deficient cells ($BRCA2^{-/-}$) expressing EGFPMBP-BRCA2 WT or VUS, as indicated.

StainFree image of the gel before transfer is used as loading control (cropped image is shown). **(c)** Co-immunoprecipitation of endogenous BUBR1 and PP2A-B56 from mitotic cell extracts of DLD1 stable clones expressing WT BRCA2 and the variant T207A. The interactions were revealed by anti-BUBR1 and PP2AC (PP2A catalytic subunit) antibodies.

(d) Top: Scheme of the double thymidine block procedure used to synchronize the DLD1 cells for analysis of chromosome alignment. Bottom: Quantification of misaligned chromosomes outside the metaphase plate in DLD1 BRCA2 deficient cells expressing BRCA2 WT or S206C and T207A variants. **(e)** Representative images of the type of chromosome alignment observed in cells quantified in (d), scale bar represents 10 µm. Statistical significance of the difference in (d) was calculated with two-way ANOVA test with Tukey's multiple comparisons test (the asterisks show differences compared to WT; ns (non-significant), $p > 0.05$, * $p \leq 0.05$, ** $p \leq 0.01$, *** $p \leq 0.001$, **** $p \leq 0.0001$). *n* in (d) indicates the number of cells counted in each cell clone from a total of 2-3 independent experiments.

Figure 7. BRCA2 VUS S206C and T207A show aberrant chromosome segregation

(a) SAC activity was measured by flow cytometry analysis of p-histone 3 expression in DLD1 BRCA2$^{-/-}$ stable clones after treatment with nocodazole for 14h (BRCA2$^{+/+}$ (n=3), BRCA2$^{-/-}$ (n=7), WT C1 (n=7), S206C A7 (n=6) and A9 (n=4), T207A B1 (n=5) and E4 (n=5). **(b)** Top: Scheme of the double thymidine block procedure used to synchronize DLD1 BRCA2$^{-/-}$ stable clones for analysis of aberrant chromosome segregation. Bottom: Quantification of cells with aberrant chromosomes segregation in the stable cells expressing BRCA2 WT, S206C and T207A, as indicated. Statistical

significance of the difference in (a) and (b) was calculated with one-way ANOVA test with Tukey's multiple comparisons test (the asterisks show differences compared to WT; ns (non-significant), p > 0.05, * $p \leq 0.05$, ** $p \leq 0.01$, *** $p \leq 0.001$, **** $p \leq 0.0001$). *n* in (b) indicates the number of cells counted in each cell clone from a total of 2-4 independent experiments. **(c)** Representative images of the type of aberrant chromosome segregation observed in the cells quantified in (b), CREST antibody is used as marker of centromere; nuclei are revealed with DAPI counterstaining. Scale bars represents 10 µm. **(d)** Representative image of methaphase spreads of the DLD1 stable clone bearing the S206C BRCA2 variant stained with CREST and counterstained with DAPI. In this example, the cell contains 45 chromosomes. **(e)** Distribution of the number of chromosomes observed in metaphase spreads of stable clones expressing S206C A7, T207 B1, or WT C1 (73-76 cells were analysed for each clone, modal number of chromosomes and percentage deviating from the mode are shown at the top; p values were calculated by Mann-Whitney two-tailed test; *** $p \leq 0.001$, **** $p \leq 0.0001$).

Figure 8. **DNA repair is not affected in BRCA2 variants S206C and T207A**

(a) Quantification of the surviving fraction of DLD1 cells expressing endogenous BRCA2 ($BRCA2^{+/+}$) or stable clones of BRCA2 deficient DLD1 cells ($BRCA2^{-/-}$) expressing GFPMBP-BRCA2 WT or the variants S206C or T207A assessed by clonogenic survival upon exposure to MMC at concentrations: 0, 0.5, 1.0 and 2.5 µM. Data are represented as mean ± SD: $BRCA2^{+/+}$ (red) (n=3), $BRCA2^{-/-}$ (gray) (n=5), WT C1 (black) (n=5), S206C A7 (blue) (n=2), T207A B1 (green) (n=4). **(b)** Quantification of the relative cell viability monitored by MTT assay upon treatment

with increasing doses of PARP inhibitor Olaparib, as indicated. The data represents the mean ± SD of three independent experiments.

(c) Model for the role of PLK1 phosphorylation of BRCA2 in mitosis (see text for details). In panels 2, 2', 3 and 3' blue blobs represent chromosomes, red cylinders represent the centrioles and orange lanes represent the spindle microtubules.

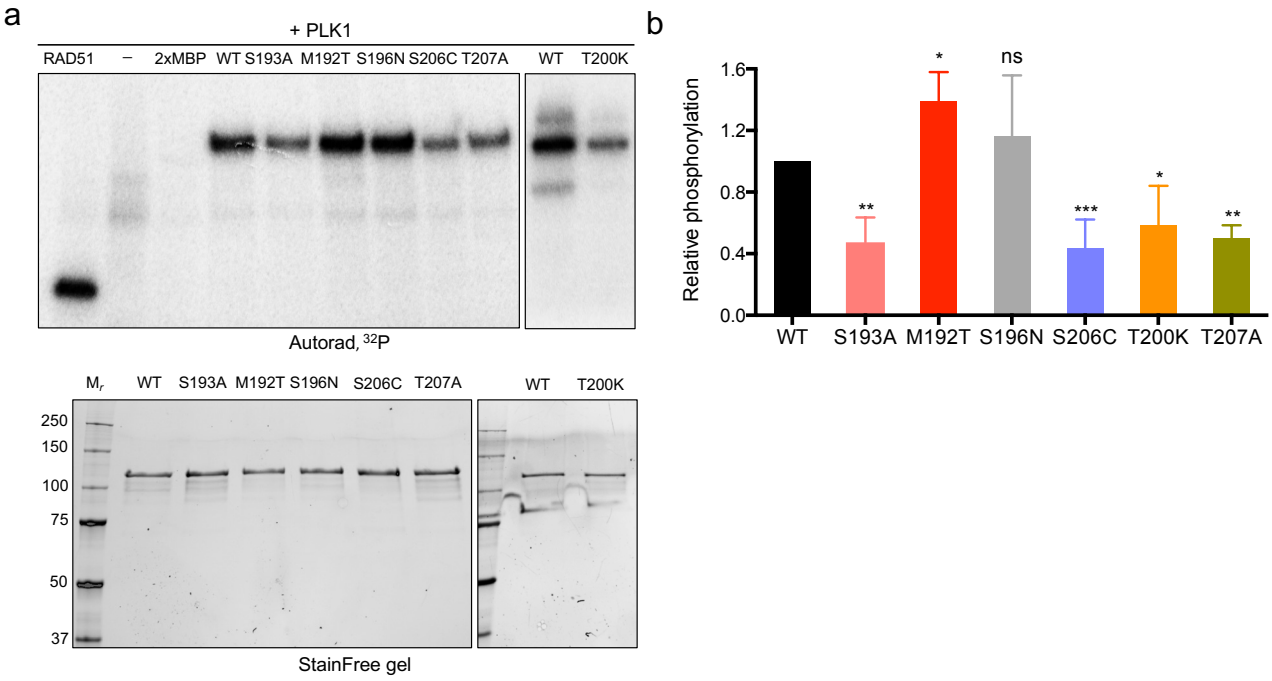
a
+ PLK1
RAD51
–
2xMBP
WT
S193A
M192T
S196N
S206C
T207A
WT
T200K
Autorad, 32P
Mr
250
150
100
75
50
37
StainFree gel
b
Relative phosphorylation
1.6
1.2
0.8
0.4
0.0
ns
*
**
***
*
**
WT
S193A
M192T
S196N
S206C
T200K
T207A

Figure 1

a

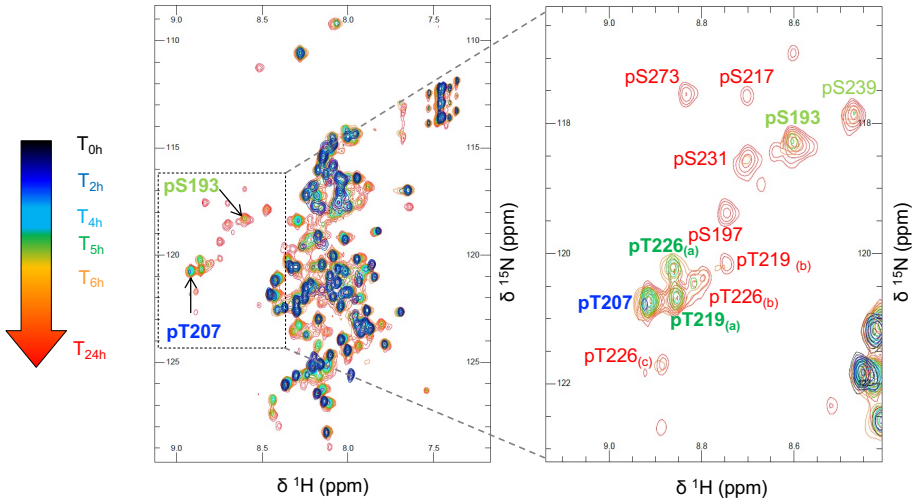
NMR: Phosphorylation kinetics (BRCA2190-283)
T0h
T2h
T4h
T5h
T6h
T24h
pS193
pT207
δ 1H (ppm)
δ 15N (ppm)
pS273
pS217
pS239
pS193
pS231
pS197
pT226(a)
pT219 (b)
pT207
pT226(b)
pT219(a)
pT226(c)

b

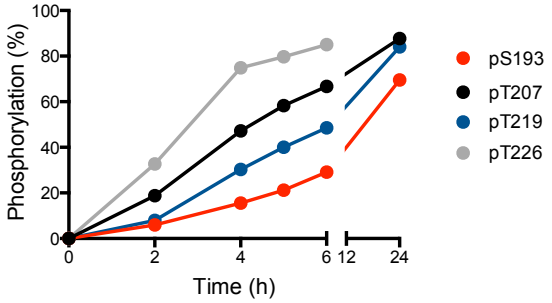
Phosphorylation (%)
Time (h)
pS193
pT207
pT219
pT226

Figure 2

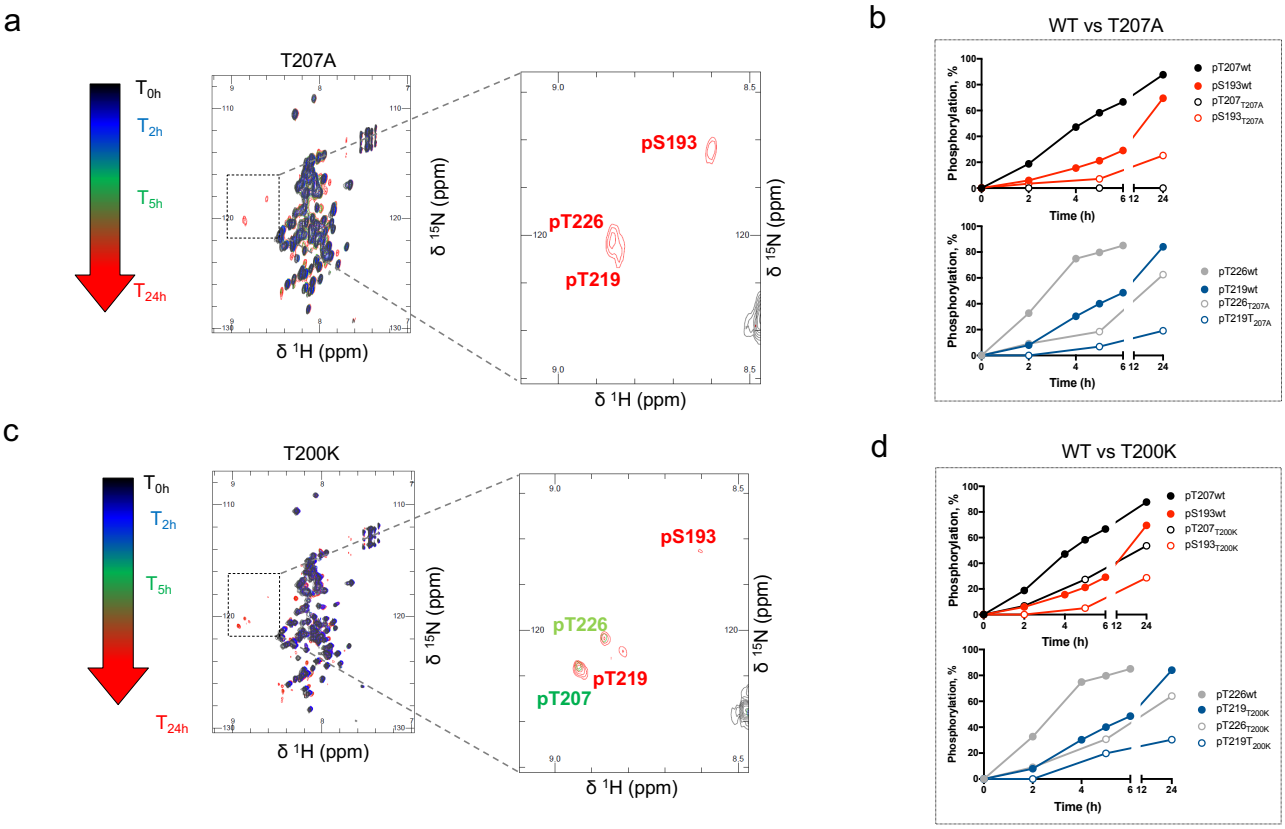
a
T207A
T0h
T2h
T5h
T24h
δ 1H (ppm)
δ 15N (ppm)
pS193
pT226
pT219
b
WT vs T207A
Phosphorylation, %
Time (h)
pT207wt
pS193wt
pT207T207A
pS193T207A
pT226wt
pT219wt
pT226T207A
pT219T207A
c
T200K
pS193
pT226
pT219
pT207
d
WT vs T200K
pT207wt
pS193wt
pT207T200K
pS193T200K
pT226wt
pT219T200K
pT226T200K
pT219T200K

Figure 3

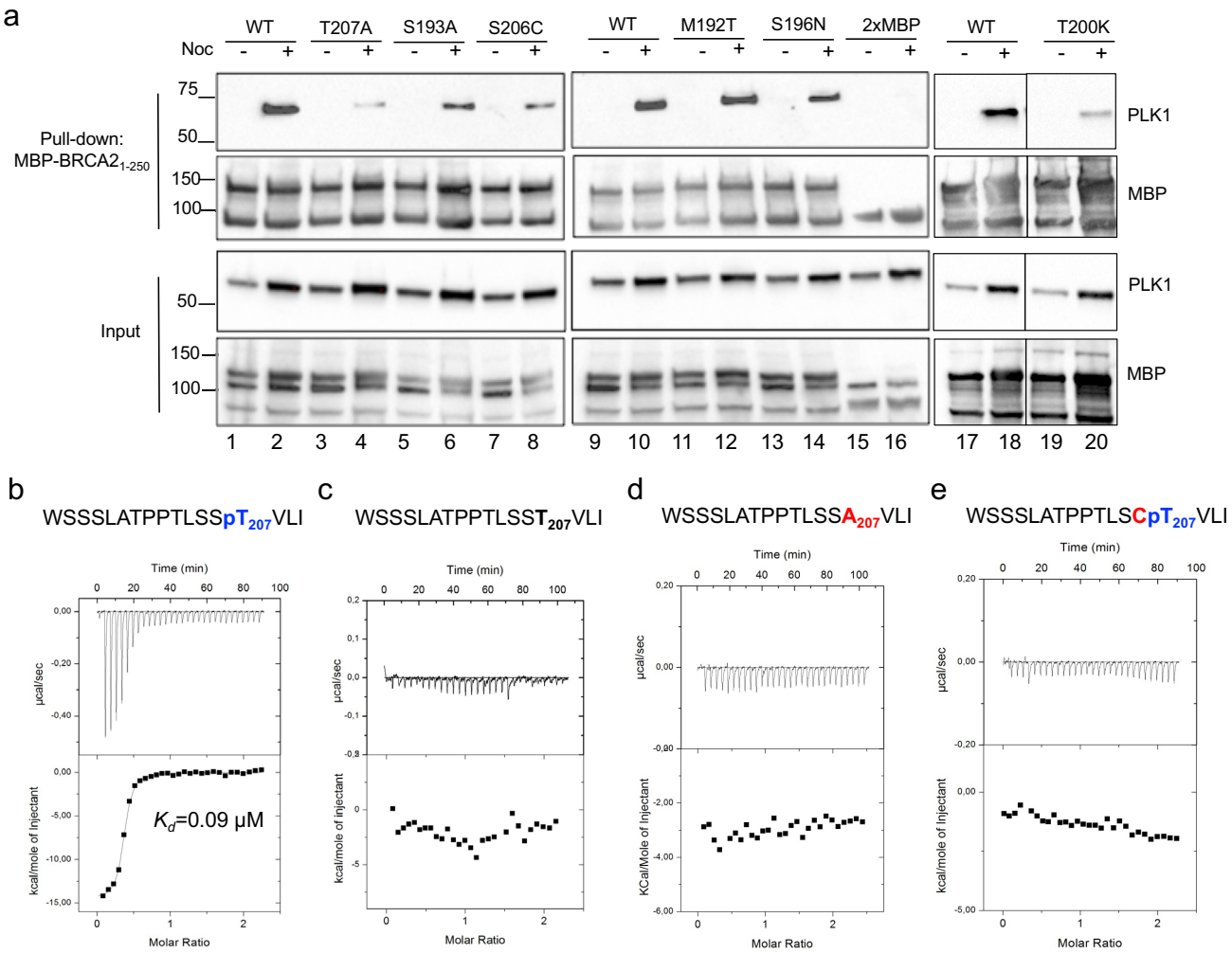
a
WT
T207A
S193A
S206C
WT
M192T
S196N
2xMBP
WT
T200K
Noc
- +
Pull-down:
MBP-BRCA2$_{1-250}$
Input
75
50
150
100
PLK1
MBP
1 2 3 4 5 6 7 8 9 10 11 12 13 14 15 16 17 18 19 20
b
WSSSLATPPTLSSpT$_{207}$VLI
c
WSSSLATPPTLSST$_{207}$VLI
d
WSSSLATPPTLSSA$_{207}$VLI
e
WSSSLATPPTLSCpT$_{207}$VLI
Time (min)
µcal/sec
kcal/mole of Injectant
KCal/Mole of Injectant
Molar Ratio
K_d=0.09 µM

Figure 4

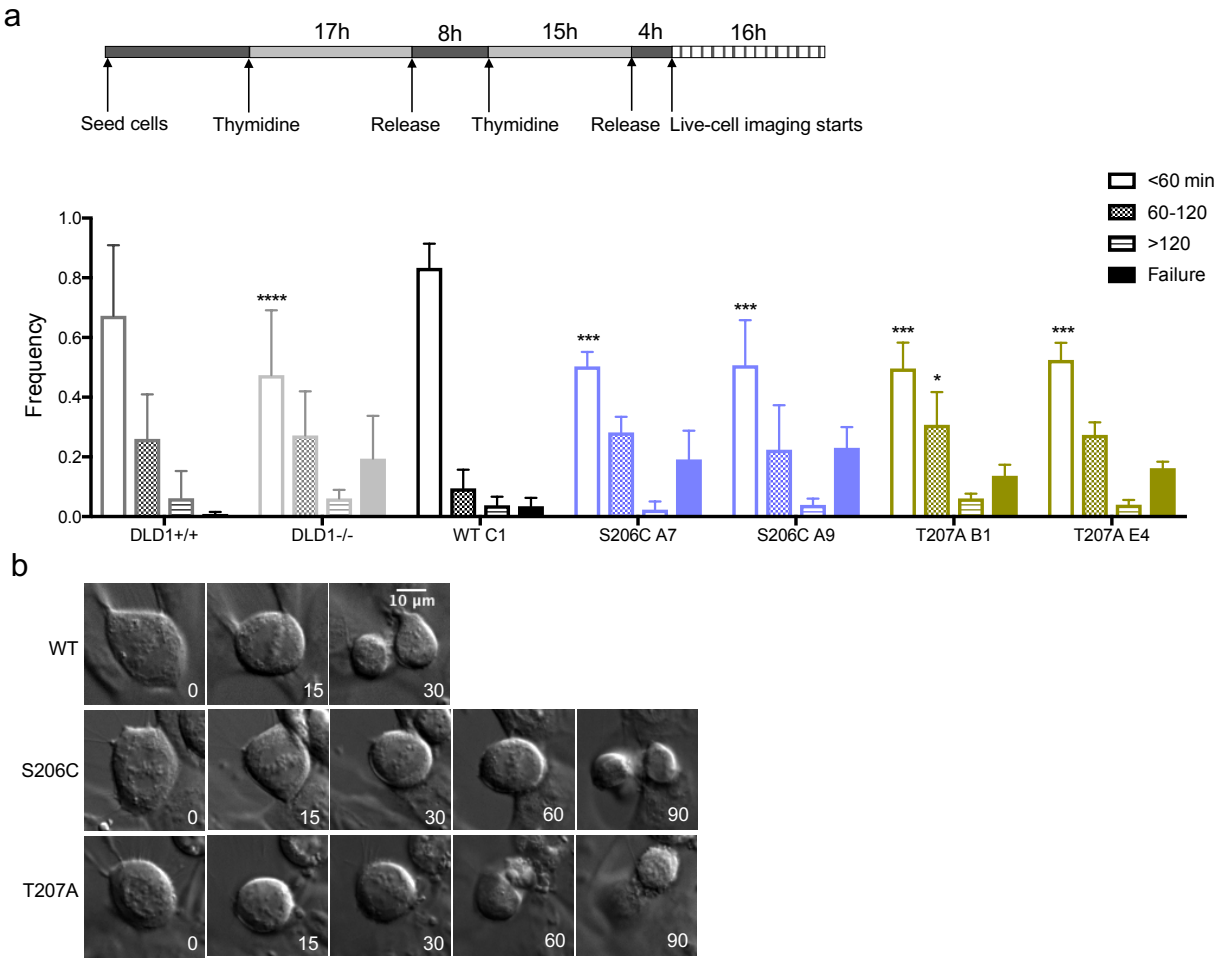
a
17h
8h
15h
4h
16h
Seed cells
Thymidine
Release
Thymidine
Release
Live-cell imaging starts
<60 min
60-120
>120
Failure
Frequency
1.0
0.8
0.6
0.4
0.2
0.0
****
***
***
***
*
***
DLD1+/+
DLD1-/-
WT C1
S206C A7
S206C A9
T207A B1
T207A E4
b
10 µm
WT
S206C
T207A
0
15
30
60
90

Figure 5

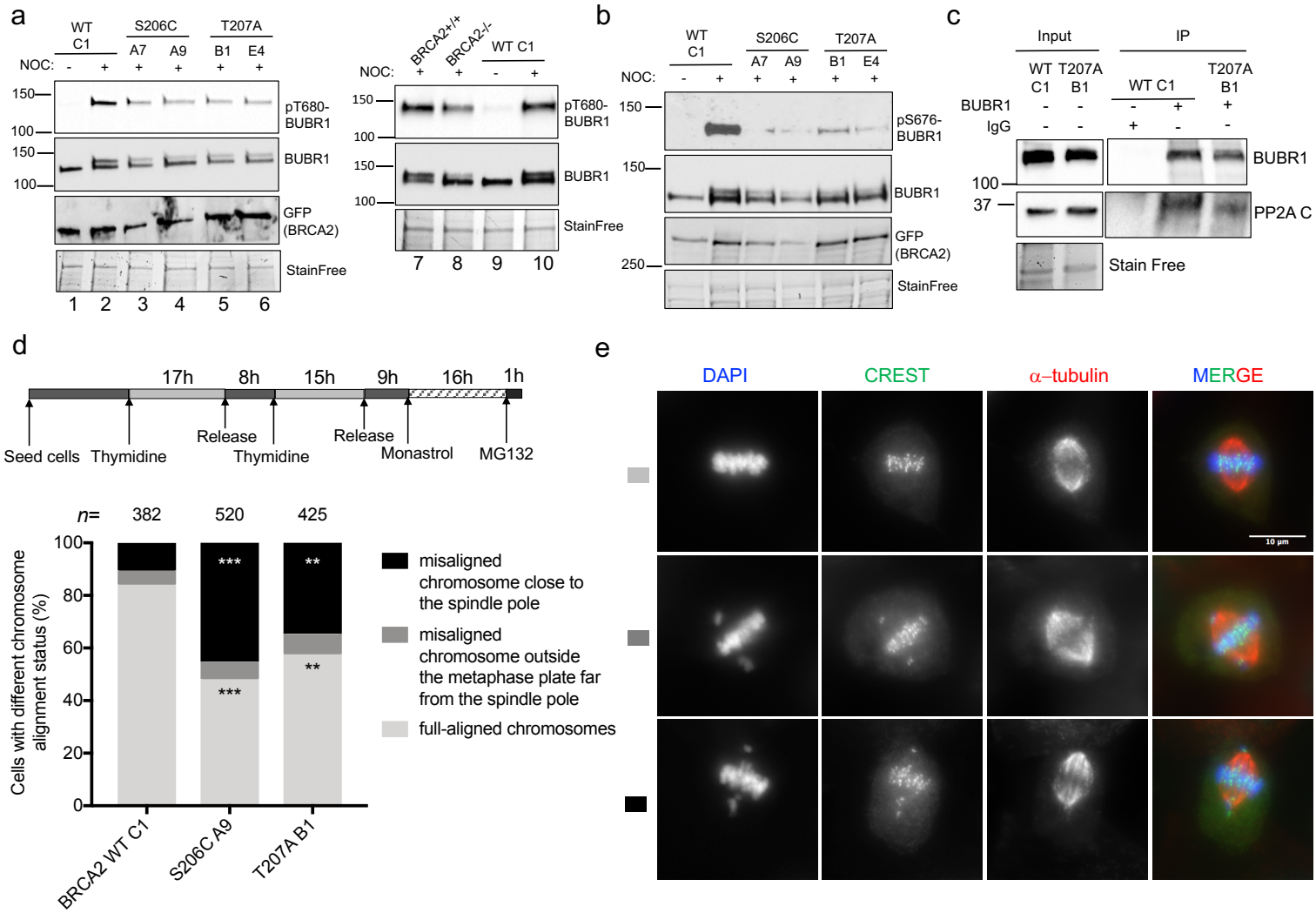
a
WT C1
S206C
T207A
A7
A9
B1
E4
NOC:
150
100
pT680-BUBR1
BUBR1
GFP (BRCA2)
StainFree
1 2 3 4 5 6
BRCA2+/+
BRCA2-/-
WT C1
7 8 9 10
b
pS676-BUBR1
250
c
Input
IP
BUBR1
IgG
37
PP2A C
Stain Free
d
17h
8h
15h
9h
16h
1h
Seed cells
Thymidine
Release
Thymidine
Release
Monastrol
MG132
n=
382
520
425
Cells with different chromosome alignment status (%)
***
**
misaligned chromosome close to the spindle pole
misaligned chromosome outside the metaphase plate far from the spindle pole
full-aligned chromosomes
BRCA2 WT C1
S206C A9
T207A B1
e
DAPI
CREST
α–tubulin
MERGE
10 µm

Figure 6

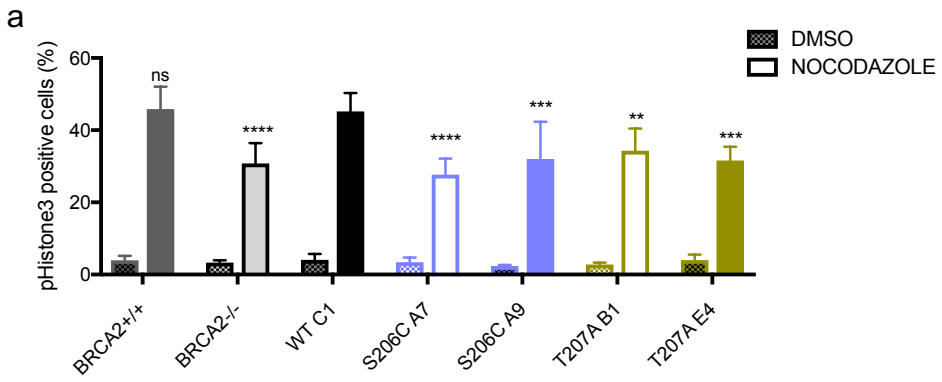
a
DMSO
NOCODAZOLE
pHistone3 positive cells (%)
60
40
20
0
ns
****
****
***
**
***
BRCA2+/+
BRCA2-/-
WT C1
S206C A7
S206C A9
T207A B1
T207A E4

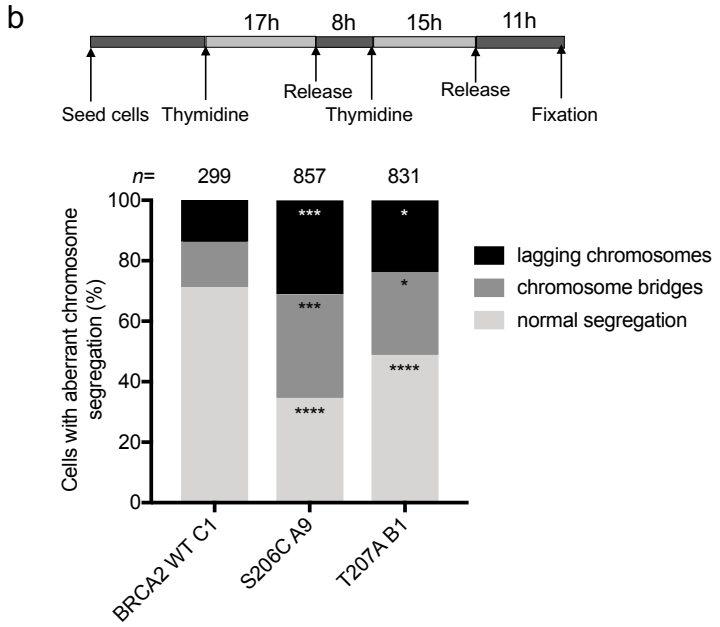
b
17h
8h
15h
11h
Seed cells
Thymidine
Release
Thymidine
Release
Fixation
n=
299
857
831
Cells with aberrant chromosome segregation (%)
100
80
60
40
20
0
***
***
****
*
*
****
lagging chromosomes
chromosome bridges
normal segregation
BRCA2 WT C1
S206C A9
T207A B1

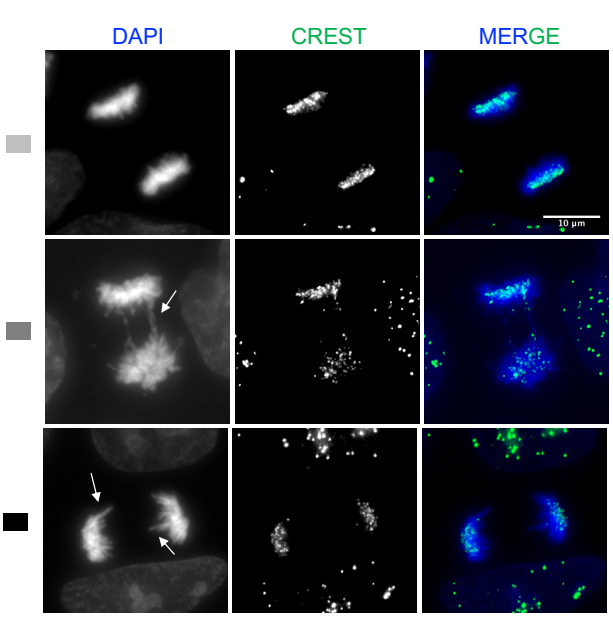
c
DAPI
CREST
MERGE
10 µm

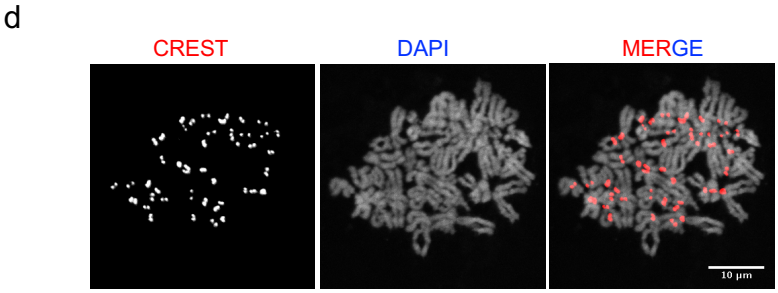
d
CREST
DAPI
MERGE
10 µm

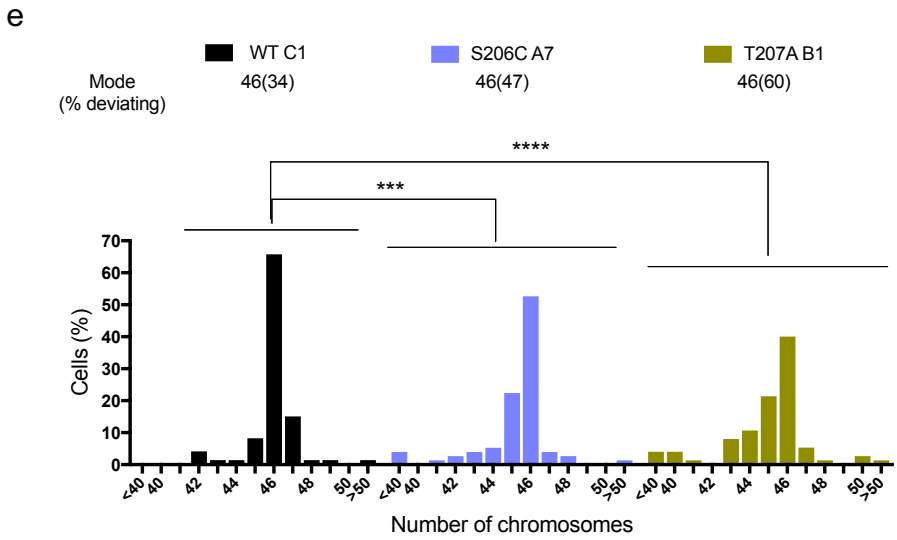
e
WT C1
S206C A7
T207A B1
Mode
(% deviating)
46(34)
46(47)
46(60)
****
***
Cells (%)
70
60
50
40
30
20
10
0
<40
40
42
44
46
48
50
>50
Number of chromosomes

Figure 7

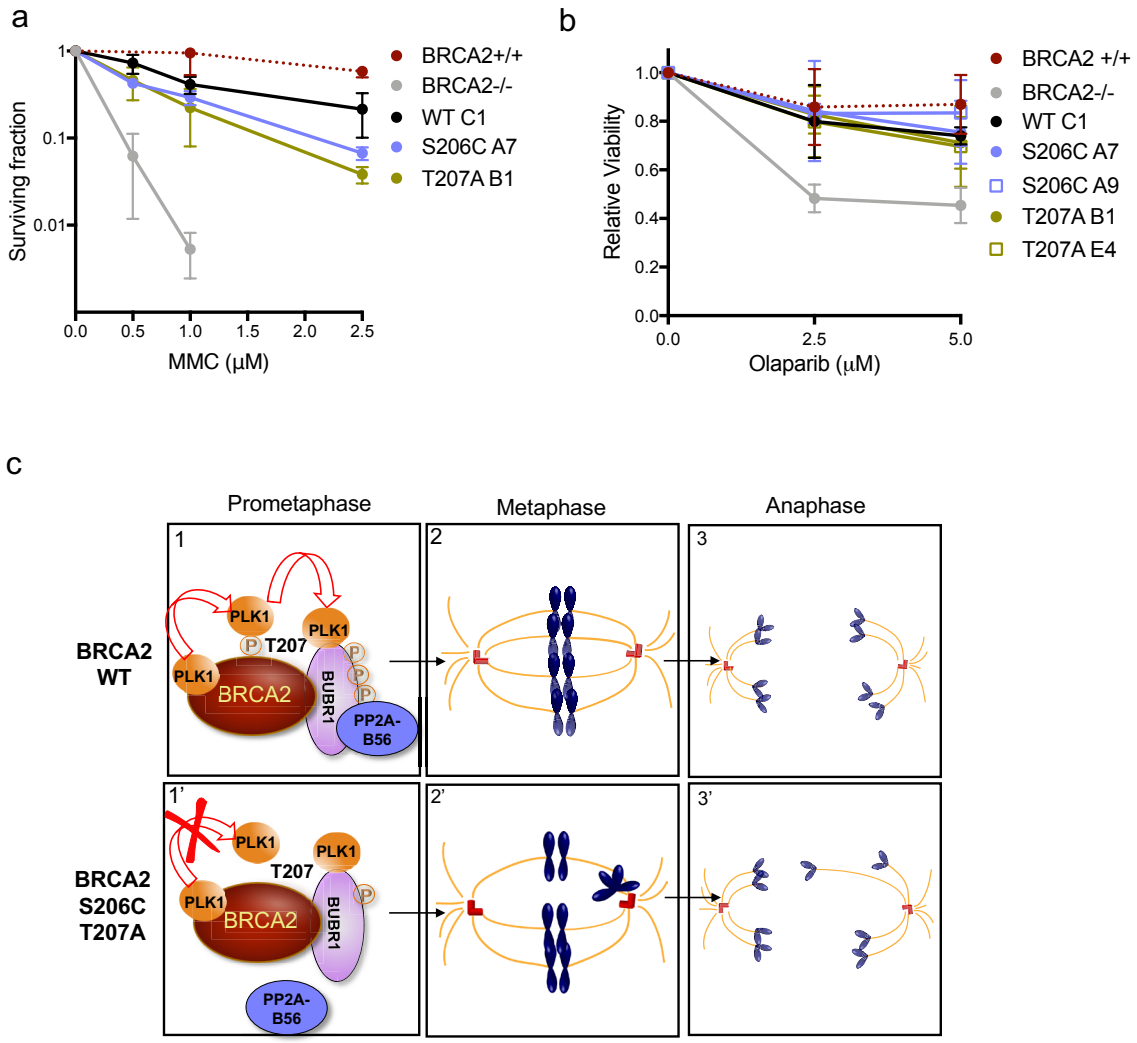
a
Surviving fraction
1
0.1
0.01
0.0
0.5
1.0
1.5
2.0
2.5
MMC (μM)
BRCA2+/+
BRCA2-/-
WT C1
S206C A7
T207A B1
b
Relative Viability
1.0
0.8
0.6
0.4
0.2
0.0
0.0
2.5
5.0
Olaparib (μM)
BRCA2 +/+
BRCA2-/-
WT C1
S206C A7
S206C A9
T207A B1
T207A E4
c
Prometaphase
Metaphase
Anaphase
BRCA2
WT
BRCA2
S206C
T207A
1
2
3
1'
2'
3'
PLK1
T207
P
BRCA2
BUBR1
PP2A-
B56

Figure 8